AIAA 95-3468, Atmospheric Flight Mechanics Conference, August 1995

VORTEX CONTROL USING A MOVEABLE NOSE WITH PRESSURE FEEDBACK

Darden, L.A.,* Peterson, K.G.,* and Komerath, N.M.†
School of Aerospace Engineering
Georgia Institute of Technology
Atlanta, Georgia 30332-0150

ABSTRACT

This paper studies the dynamic rolling moment induced on a wing-body configuration at high angle of attack by dynamic lateral asymmetry of the forebody vortices. A moveable nose tip is used to rapidly induce and control lateral asymmetry of the forebody vortices. The configuration is constrained in roll so that the measurements are performed at zero bank and sideslip angle. The difference in surface pressure across the Zero Vorticity Contour of the forebody vortices is used as a sensor of asymmetry. Correlations between nose motion, wing rolling moment, and pressure difference are examined. Square wave and sinusoidal nose motions are used, at frequencies from 0.1 to 1 cycle per second. Long-period square waves and sine waves are used to confirm the time lags for the pressure and the moment. Adverse yaw-roll coupling is observed at 40+ degrees incidence. At 35 degrees and lower, the initial moment effect is followd by a slower-developing, counteracting moment. This difference is attributed to the effect of vortex bursting or multiple states of wing flow separation. Surface pressure feedback is seen to be a viable method of controlling rolling moment, with the presure on the forebody responding with a very short time scale to the nose motion. The time lag in roll moment response is seen to be an order of magnitude longer than the freestream convection time, and the anomalous moment effect to take another order of magnitude longer. Steady state moment variations with nose position are consistent with the adverse roll-yaw coupling at 40 and 45 degrees incidence, whereas the counteracting moment effects greatly reduce the moment sensitivity at 35 degrees and lower incidence. The experiments indicate the presence of at least three widely different time scales in the roll-yaw coupling of maneuvering aircraft, visible even in roll-constrained experiments.

* Graduate Fellow. Student Member, AIAA
† Professor. Associate Fellow, AIAA.

NOMENCLATURE

Cm:	rolling moment coefficient based on mean aerodynamic chord.
ZVC:	Zero Vorticity Contour, separating vortex systems on the two sides of the forebody.
α:	angle of attack.
ϕ:	body azimuth where ZVC intersects, in degrees from plane of lateral symmetry.
θ:	Nose tip deflection from the plane of lateral symmetry, deg., positive to the right of the model.

INTRODUCTION

The dynamics of the forebody vortex system are of interest in controlling the yawing and rolling moments on aircraft which maneuver at high angles of attack[1-5]. In this paper, we explore the effect of forebody vortex asymmetry on the vortex system over the wings, and the resulting effect on the rolling moment experienced by the aircraft. A roll-constrained experiment enables us to isolate the vortex-induced roll moment without contamination from the roll moment due to sideforce on a yawed or banked forebody, and thus to examine the different time scales of the problem. Surface pressure feedback is used as an independent measure of vortex asymmetry and its effects on rolling moment.

In ref. 6 we demonstrated the use of the moving stagnation point, using a small conical nose tip, to control vortex asymmetry. Figs. 1 and 2 show the wing-body model and its moveable nose tip[6]. Static control of forebody vortex asymmetry was demonstrated, and the dynamic relationship between nose position and vortex asymmetry was measured from video images using a transfer function approach. The lag for the vortex response to reach the wings was an order of magnitude longer than the freestream convection time.

The results of Ref. 6 were obtained by labor-intensive analysis of video images obtained by laser sheet flow visualization of smoke in cross-flow planes, and of the shadow of the moving nose.

As a diagnostic of asymmetry, the intersection point on the fuselage surface of the Zero-Vorticity Contour (ZVC) dividing the vorticity associated with the vortices on either side of the forebody was used. Success in correcting static asymmetry[6] is shown in Fig. 3. The time traces of the ZVC deflection and the nose deflection, obtained from analyzing video sequences, were sampled and used to generate frequency-domain auto- and cross-spectra. The transfer function between the output (ZVC deflection) and the input (nose deflection) was computed, as shown in Fig. 4. The coherence function (Fig. 4a) was used to determine frequency values where a linear, causal relationship existed between the input and output. The magnitude of the transfer function at these frequencies (Fig. 4b) was used to compute the sensitivity of the ZVC to nose deflection at each frequency, and extrapolated to get the steady-state sensitivity. This indicated that the sensitivity increased with frequency (rate) of the nose motion, as might be expected from considerations of "moving-wall effects" on the boundary layer velocity profiles[1-3]. The phase of the transfer function (Fig. 4c) in the range of high coherence was found to be linear, and enabled extraction of the delay time between nose motion and vortex response.

The time lag was found to be extraordinarily long, an order of magnitude larger than the freestream convection time. The lag was confirmed by direct examination of the videotape, and grew much faster than the convection time as indicated by the results obtained at a cross-section further downstream over the wings. The experiments of Ref. 6 were confined to the low wind speed (1-3 m/s) required for good flow imaging. Surface pressure measurement was not feasible at such low dynamic pressures.

The ZVC was shown to be a successful diagnostic of forebody asymmetry, linearly and coherently related to the nose position, for fairly significant levels of nose deflection and asymmetry, at the upstream position. Further downstream, where the wing vortex system dominated the flow images, such coherence and linearity were not obtained. In fact, video images obtained far downstream, and those obtained in Ref. 7 indicate that the presence of vortex bursting would reverse the significance of the ZVC. This is seen later in this paper.

OBJECTIVES

In this paper we examine the effect of the moving nose on the rolling moment induced on the wing-body model. Further, we examine the feasibility of using surface pressure signals to provide real-time feedback on the asymmetry, so that the rolling moment can be controlled. The phase relationships between nose movement, pressure, and rolling moment are demonstrated. Actual use of the pressure feedback for roll control is deferred to later work for reasons seen from the following: there were much more interesting issues seen during the investigation.

ISSUES

Previous work has focused on controlling forebody vortex asymmetry[4,5] and dynamic phenomena such as wing rock, where all the time scales of the problem are active simultaneously. Control of wing rock has been demonstrated by turning forebody blowing on and off[8]. High-rate, pulsed control of the forebody vortex system had not been demonstrated.

1) Time Lag for Pressure and Moment Response
The time delays in the development of the pressure and the moment are important features of a complete control system, and are distinct from those due to aircraft inertia.

2) Complexity of Steady-State Response
Quasi-steady control is complex in the presence of the multiple roll states[9,10].

3). Sensing the ZVC Using Surface Pressure
To extend the ZVC concept to a feedback sensor, an alternative had to be found to the laborious process of analyzing cross-flow video images. In this paper, we use the pressure signature under the forebody vortex system (Fig, 5). Five potential questions arise about this:
a). whether the pressure gradient near the ZVC is sufficient to sense accurately in low-speed tests;
b). whether the presence of secondary or tertiary vortices would cause non-unique pressure signatures as the ZVC moved;
c). whether static pressure sensors, with their long tubes, have fast-enough response to be useful;
d). whether the pressure difference would be non-unique because of the ZVC skipping entirely out of the region between the pressure sensors; and
e). whether unsteady pressure sensors will have adequate sensitivity for low-speed experiments, and whether they will have a frequency response at low-enough frequencies to allow quasi-steady tests.

Answers are found to some of these questions in this paper. Questions d) and e) were avoided and deferred to later work. Surface pressure feedback proved useful as a measure of asymmetry and correlated with the rolling moment.

4) Need for Roll-Constrained Experiments

On a free-flying aircraft at angle of attack, lateral asymmetry at the nose has two effects, as shown in Fig.6. First, there is a sideforce at the nose, which induces airplane yaw. In turn, this causes a rolling moment. Once the airplane is at a non-zero bank angle, the rolling moment is coupled to the forebody yaw and sideforce. The sensitivity of roll moment to bank angle is complex and non-monotonic[9,10]. Secondly, the asymmetric forebody vortices interact with the wing vortices, and induce asymmetry over the wings, causing a rolling moment. The time scales for these two processes may be very different. The pressure difference at the very tip of the forebody, and hence the yawing moment, may develop very rapidly, whereas the vortex-induced wing asymmetry may take a long time, as indicated by the results of Fig. 4 and Ref. 6. Thus it is important to separate out the two processes in this experiment. This is done by constraining the model in roll: a strain-gauge roll balance was designed which allows less than 0.25 deg. roll at the moments measured, and was proven to be insensitive to side forces.

TEST CONFIGURATION

The experiments were performed in the 42" by 42" Low Speed Wind Tunnel at the School of Aerospace Engineering. The tunnel speed can be varied between 5 and 70 ft/s, measured with a pitot static probe. The model has a 60 degree delta wing with cylindrical fuselage and a body-of-revolution nose terminating in a conical nose tip (Fig. 1). The conical nose tip has a semi-apex angle of 15 deg. and a length of .03 m, compared to the model length of 0.77 m. A servo motor installed in the fuselage rotates the nose in the yaw plane. The axis of rotation of the servo is along the yaw axis of the model and thus servo actuation induces no rolling moment on the model, as verified in wind-off tests. The servo motor is controlled through a data acquisition board in an Intel 486-based computer and moves the nose tip through maximum yaw angles of ±10 degrees. This corresponds to a maximum lateral deflection of the nose tip by 8.1 mm.

The model is stingmounted with a steel rod along the roll axis. Angles of attack between 18° and 45° are possible (Fig. 7). A moment balance attached to the sting uses flexures and strain gages to measure the instantaneous rolling moment of the model. The balance was calibrated by applying a series of known moments using weights and pulleys.

Two basic sets of experiments were conducted for this paper. The first examined the response of the model rolling moment to excitation of the nose; the second examined the feasibility of utilizing the moving nose tip as a control device to maintain a certain commanded roll moment, in anticipation of future free-to-roll experiments. In the second set of experiments, static pressure taps are used to measure the roll moment and are correlated to the data from the rigid balance. The static pressure taps were drilled at 70 deg. from the vertical on each side of the fuselage, with the foremost pair drilled into the wooden portion of the forebody, 140mm from the nosetip. The model was rigidly mounted to the moment balance at zero yaw and bank angle and tested at α = 20°, 30°, 35°, 40°, and 45°. Data at 45, 50, 55, 60 and 65 ft/sec. were obtained at each α.

At each angle of attack, 3 tests were performed. First the model was subjected to a step function change in nose tip angle. Roll moment data was obtained and recorded for 10 seconds at a sampling rate of 100 Hz. The data for each nose tip angle was averaged to obtain a static roll moment corresponding to the given nose tip deflection. The other 2 experiments examined the roll moment response to square wave and sine wave excitation of the nose tip. Frequencies of 0.1, 0.5 and 1Hz were used to excite the system, and roll moment data was taken for periods and sampling rates as outlined in Table 1.

Table 1: Sampling Parameters for the Square and Sine Wave Nose Deflections

Wave Frequency	Sampling Rate	Sampling Time
1.0 Hz	100 Hz	20 seconds
0.5 Hz	100 Hz	30 seconds
0.1 Hz	100 Hz	60 seconds

The second series of tests was conducted with 4 pairs of static pressure taps installed in the nose and body of the model. The test series sought to determine the utility of pressure feedback data for use in a closed loop controller. The taps were positioned 70° from the vertical axis of symmetry at stations 140, 160, 190, and 240 mm aft of the nose tip. Data was obtained at α = 35° for each set of pressure taps for the tunnel speeds and frequencies used for the moment only tests. The sampling rate and nose update rate also remained unchanged. As before, the model was restricted from rolling, thus eliminating the effect of model dynamics on the data. To meet the Proceedings Deadline, only the data from the first set of pressure taps was completely analyzed. In order to clarify time lag and phase lag another series of tests was conducted with the nose initially held at zero deflection and then moved through one period of desired oscillation. Single period tests were

conducted at 45, 55, and 65 ft/sec, for nose oscillation frequencies of 1, 0.5, 0.2 and 0.1 Hz.

Measurement Uncertainty

The strain gage balance allowed no more than 0.25 degrees roll at the highest moments measured in this paper. The uncertainty in moment measurement was 1%. The frequency response of the strain gage circuitry was flat far beyond the range of interest. Static pressure difference was measured using a Barocel with a range of 10 mm Hg and a least count of one part in 10^6 of sensor range. The uncertainty in the measured values was 0.15 %. The response of the static pressure measurement system was calibrated as follows: pressure was sensed through tubes of the same length as used in the experiment: approximately 1500mm. The two tubes were connected across a Scanivalve pressure switch, with a pressure difference applied across it. By switching ports, a step pressure difference was applied. The decay time was measured, and the time constant determined. The value was .09 seconds, comparable to the time for one pass of the pressure pulse and its reflection to traverse the tube at the speed of sound. This time constant thus allows reliable sensing of pressure variations up to at least 5Hz, adequate for use in controlling the moment. However, the delay time of 0.09 second is significant in interpreting the time lag of the pressure in comparison to that of the moment, when the nose is deflected. All "nose deflection" data presented are the input waveforms: that the nose responds faithfully is confirmed by examining the pressure data later.

RESULTS

1. Moving the nose causes a rolling moment at zero bank angle.

At zero bank angle, rolling moment must come from vortex interaction. The dynamic data will be presented first. Fig. 8(a) shows that a sinusoidal nose oscillation at $\alpha = 40°$ with a period of 10 seconds and an amplitude of 10 deg. produces a roll moment coefficient with an amplitude of 0.075. This is comparable to or larger than the moment coefficients achieved in the wing rock experiments of Ref. 8 using forebody blowing and the vortex control experiments using nose strakes in Ref. 4. As the sine wave frequency increases, the phase shift changes, and the amplitude of the response decreases somewhat. This is seen from Fig.8(b) and (c), where sinusoidal nose motions of 0.5 and 1Hz are applied.

2. Moment Responds to Square Wave Nose Motion

Figure 9 shows the roll moment response to square wave motion of the nose at various frequencies. Again, the amplitude is 10 deg. and the frequencies tested are 0.1, 0.5 and 1 Hz. Fig. 9(a) shows that the nose does indeed execute sharp oscillations, as seen from the sharpness of the leading edge of the moment waveform. This feature makes the moving nose a useful tool for basic studies of vortex dynamics. The opposite signs of the nose movement and the rolling moment correspond to the adverse yaw-roll coupling expected. Figs. 9(b) and(c) shows the response of the rolling moment to square waves at higher frequency: substantial response lag is seen, though the amplitude is not attenuated any more than in the sine wave case.

3. Anomalous Moment Characteristics at $\alpha = 35$.

Fig. 10 shows the corresponding results of sinusoidal nose motion at $\alpha = 35$ deg. The moment response is much lower in amplitude than at $\alpha = 40$ deg. at all 3 frequencies. The phase lag is much more significant than at 40 deg. as well. We next look at the response to square wave excitation. In Fig. 11(a) the response to a square wave at 0.1Hz begins with the moment moving opposite to the nose, as expected from the adverse yaw-roll coupling discussed before. However, this is soon followed by a reversal of the moment. This accounts for the overall attenuation of the roll response, seen in the sine wave case of Fig. 10. The reason for this behavior is not known from these experiments. However, it may be postulated from previous work on wing rock and delta wing roll that unsteady vortex bursting and multiple states of flow separation are responsible for this behavior.

4. Asymmetry sensed using surface pressure

Fig. 12 shows the pressure difference between the two sides of the forebody, measured at the station 140 mm from the nose, compared with the wing rolling moment. Fig. 12(a) shows a sinusoidal nose motion at 0.5Hz at $\alpha = 35$ deg. The first observation is that the surface pressure trace is indeed well correlated with the nose motion and thus is a successful sensor of asymmetry. Secondly, we see that even at $\alpha = 35$ deg., a sinusoidal nose motion produces a sinusoidal pressure variation. The variation is what is expected based on the nose/vortex correlation seen in Ref. 6 and in the moment response at $\alpha = 40$ deg. The moment response at 35 deg., however is complex: this strengthens the postulate of vortex burst or other dynamic response of the wing vortex system induced by dynamic asymmetry of the forebody vortices. Again, we note that the aircraft is immobile, and bank angle is well under 0.25 deg.; however, the wing vortex system can jump to another "state" because of the induced asymmetry.

In Fig. 12(b), we examine the response to a square wave at 0.1 Hz under the same conditions as before. Again we see that the surface pressure response is quite normal, and the pressure reacts to the sharp change in nose angle. However, the moment response, as seen before for the 35-deg. case, starts with a blip in the right direction, but then reverses, so that the overall plot looks like a derivative-type response. Again, this strengthens the hypothesis that this anomalous response is a wing vortex effect, present only in a restricted range of angle of attack.

Steady-State Behavior

Unfortunately, the steady-state behavior of the vortex system is more difficult to interpret. Fig. 13 shows the quasi-steady moment cofficient vs. nose position for various speeds. The data are complex. The data at α of 40 and 45 deg. are fairly consistent, with the slope of the curve at zero nose deflection being what is expected. The failure to collapse all the curves obtained at different speeds is troubling and perhaps indicative of Reynolds number effects in the vortices. This is contrasted with the dynamic moment data in Figs. 8 -10: the moment coefficient is indeed independent of flow velocity there. However, the data at 35 deg. (and lower angles of attack) show complex moment behavior: again, we attribute this to the additional effect of wing vortex instabilities.

Multiple Time Scales

Close examination of the pressure traces obtained at various speeds (like Fig. 12) shows a time lag of approximately 0.1 seconds, while the moment lags by approximately 0.2 seconds. Fig. 14 shows our calibration of the pressure sensor response. A sudden jump in pressure was imposed using two supplies connected to the input of a Scanivalve™ solenoid pressure switch. The response measured by the Barocel sensor indicates a system time lag of approximately 0.09 seconds. When this is taken into account, the pressure response to nose motion in Fig. 12 is essentially instantaneous. The 0.2 second lag in the moment response is real, because the frequency response of the moment measuring system is far higher than this. The lag in moment response is also much higher than the freestream convection time, which is on the order of 0.02 seconds. This isolates and demonstrates the existence of a long vortex time scale in the dynamics of a rolling aircraft. In addition, we saw that the wing vortex dynamics can have another longer time scale at the 35-deg. (and lower α cases).

DISCUSSION

Ref. 6 showed that moving the nose to the right would move the ZVC to the left, at 25 deg. incidence. This indicates that the stronger vortex, closer to the surface is on the side to which the nose moves, and is consistent with expectations based on the stagnation point hypothesis: the boundary layer on the favored side starts off with a much more favorable velocity gradient, and the vortex lifts off much later, than on the "windward" side (left side in this case). According to this explanation, the suction on the right side of the forebody should increase, causing a side force to the right. As the stronger vortex on the right side merges with the wing vortex, the lift on the right wing should go up, causing a rolling moment to the left. This is an adverse roll-yaw coupling, as is observed at the 40 deg. and 45 deg. cases.

For α = 35 deg., the roll response is less sensitive to nose deflection, and the sense of the response is opposite to the 40 and 45-deg. cases. Our explanation is that we get into the unsteady vortex bursting regime or multiple "roll states"[9,10] at this angle of attack. This conclusion is supported by comparison of pressure and moment data in Fig. 12, and is reinforced by examination of the static moment data of Ref. 13. The time lag for the development of this counteracting phenomenon is seen to be much longer than that for the initial moment response. Again, this corresponds to the observations of Ref. 9, where time lags up to 2 orders of magnitude longer than the freestream convection time were reported for the multiple states encountered in the roll response of a delta wing vortex system.

Thus we have shown the existence of three different time scales in the dynamics of a maneuvering aircraft, present even when the aircraft is constrained to be at zero bank angle:

1. The short time scale for pressure asymmetry to develop on the forebody due to vortex asymmetry triggered at the nose stagnation point.
2. A time scale as much as one order of magnitude higher, for the moment on the wings to start responding to the vortex asymmetry, probably due to the long time it takes for the vortex asymmetry to reach the wings
3. A time scale another magnitude longer, for other dynamics of the wing vortex system to take effect, given the initial moment perturbation due to the asymmetric forebody vortices.

Other time scales due to the development of effective aircraft yaw due to bank angle, and the inertia of the aircraft itself, will come into play in free-to-roll and free flight tests.

CONCLUSIONS

We have shown that the moving nose is a successful device to produce vortex-induced rolling moment on the wings and allowing isolation of specific time scales for basic studies. We have used this feature to explore the various time scales involved in the dynamics of a maneuvering aircraft, beginning with a roll-constrained experiment. Several conclusions can be drawn:

1. Rolling moments obtained using the moving nose are comparable in magntitude to (actually larger than) those achieved using forebody blowing and rotatable strakes.
2. Sharp, controlled square-wave oscillations of the nose are demonstrated, with corresponding response characteristics of pressure and moment.
3. Static pressure difference can be used as an effective feedback sensor of forebody vortex asymmetry.
4. Static pressure difference on the forebody is seen to develop essentially instantaneously when the nose is deflected.
5. There is a substantial time lag in the development of the rolling moment due to forebody vortex asymmetry, an order of magnitude longer than the freestream convection time.
6. Vortex-induced roll moment at high angles of attack conforms to the expected adverse yaw/roll coupling.
7. At lower angles of attack, the initial roll moment induced by forebody vortex interaction appears to trigger other dynamics of the wing vortex system with counter-acting effects.
8. The time scale for these phenomena is much longer than that for the initial moment response, conforming to results reported for multiple states on rolling delta wings.

ACKNOWLEDGEMENTS

This work was performed under AFOSR AASERT Grant F49620-93-1-0342, monitored by Maj. Daniel Fant and Dr. Len Sakell. The first author receives support from an NSF Graduate Fellowship, and the second from a Mercury Seven Foundation Fellowship. Assistance from John C. Magill and other members of the Experimental Aerodynamics research team is gratefully acknowledged.

REFERENCES

1. Ericsson, L.E. and Reding, J.P., "Asymmetric Vortex Shedding from Bodies of Revolution", *Tactical Missile Aerodynamics*, Vol. 104, 243-296.

2. Ericsson, L.E. and Reding, J.P., "Dynamics of Forebody Flow Separation and Associated Vortices", *Journal of Aircraft*, Vol. 22, No. 4, April, 1985, p. 329-335.

3. Ericsson, L.E., "Sources of High Alpha Vortex Asymmetry at Zero Sideslip", *Journal of Aircraft*, Vol. 29, No. 6, Nov.-Dec., 1992, p. 1086-1090.

4. Suárez, C., Malcolm, G., and Ng, T., "Forebody Vortex Control With Miniature, Rotatable Nose-Boom Strakes", AIAA 92-0022, January, 1992.

5. Brandon, J.M. and Nguyen, L.T., "Experimental Study of Effects of Forebody Geometry on High Angle-of-Attack Stability", *Journal of Aircraft*, Vol. 25, No. 7, July, 1988, p. 591-597.

6. Darden, L.A. and Komerath, N.M., "Forebody Vortex Control At High Incidence Using A Moveable Nose Stagnation Point", AIAA 95-1775, Proceedings of the 13th Applied Aerodynamics Conference, June 1995.

7. Komerath, N.M., Liou, S-G., DeBry, B., Lenakos, J., "Measurements Of The Unsteady Vortex Flow Over A Wing-Body At Angle Of Attack", AIAA 92-2729, June 1992.

8. Celik, Z.Z., Pedreiro, N., and Roberts, L., "Dynamic Roll and Yaw Control by Tangential Forebody Blowing", AIAA-94-1853, June 1994.

9. Huang, X.Z., Hanff, E.S., Jenkins, J.E., and Addington, G., "Leading-Edge Vortex Behavior on a 65° Delta Wing Oscillating in Roll", AIAA 94-3507, August, 1994.

10. Jobe, C.E., Hsia, A.H., Jenkins, J.E., and Addington, G.A., "Critical States and Flow Topology on a 65° Delta Wing", AIAA 94-3479, August, 1994.

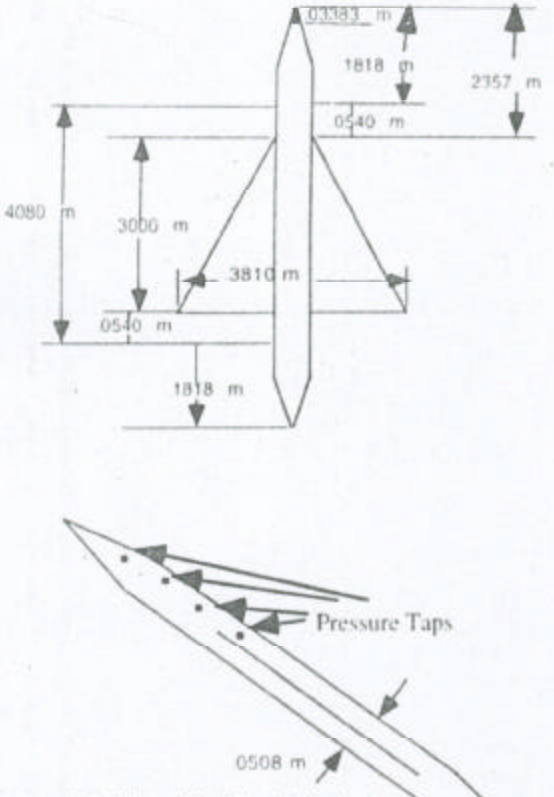

Figure 1. 60 deg. Delta Wing Model with Body of Revolution Fuselage and Moveable Nose Cone

Figure 2. Boundary layer originates with an asymmetry because the nose tip stagnation point is displaced from the plane of lateral symmetry by a geometric defect. (Reference 6)

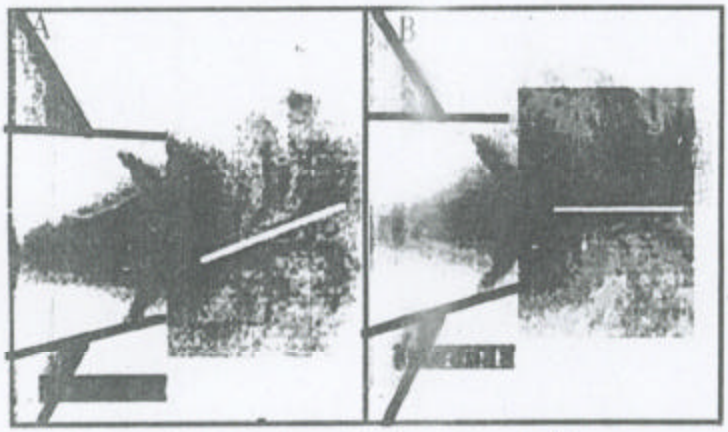

Figure 3. Example of Correction of Steady Asymmetric Vortex Patterns over the Forebody by Motion of the Nose Tip. (A) Asymmetric at 40 deg. angle of attack. (B) Symmetric at 40 deg. Image enhanced for gray-scale paper printing. (Reference 6)

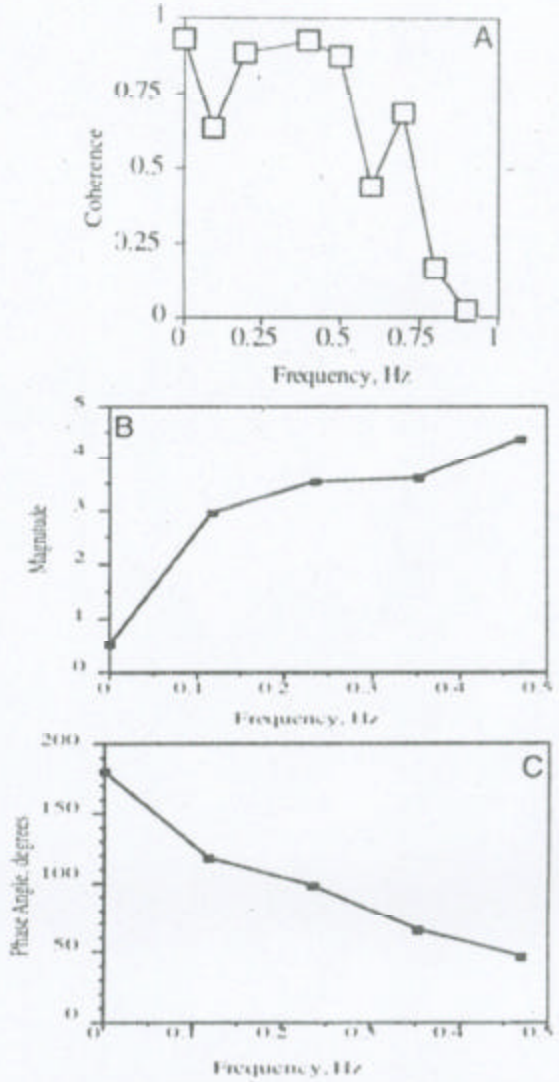

Figure 4. Transfer Function and Coherence Between ZVC Response and Nose Deflection. a) Coherence, b) Magnitude, and c) Phase Angle (Reference 6)

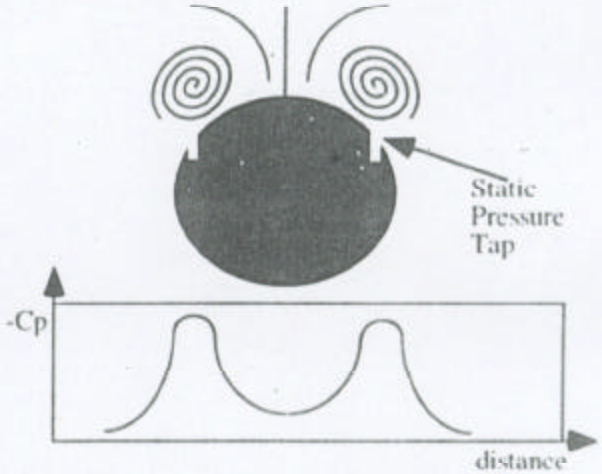

Figure 5. Surface Pressure Variation Across a Forebody at Angle of Attack and its Use in Sensing Asymmetry

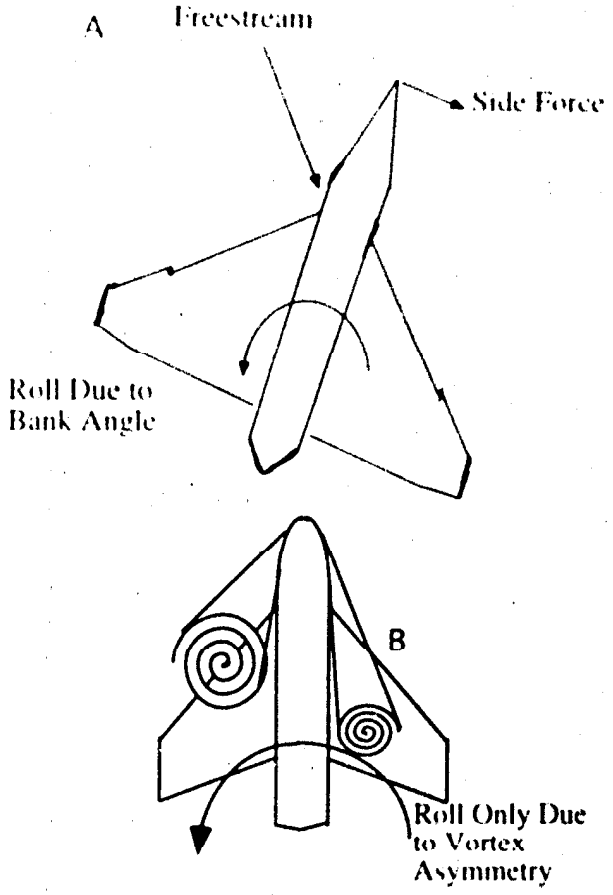

Figure 6 Sources of Roll Moment on an Aircraft at a) non-zero bank angle and b) zero bank angle

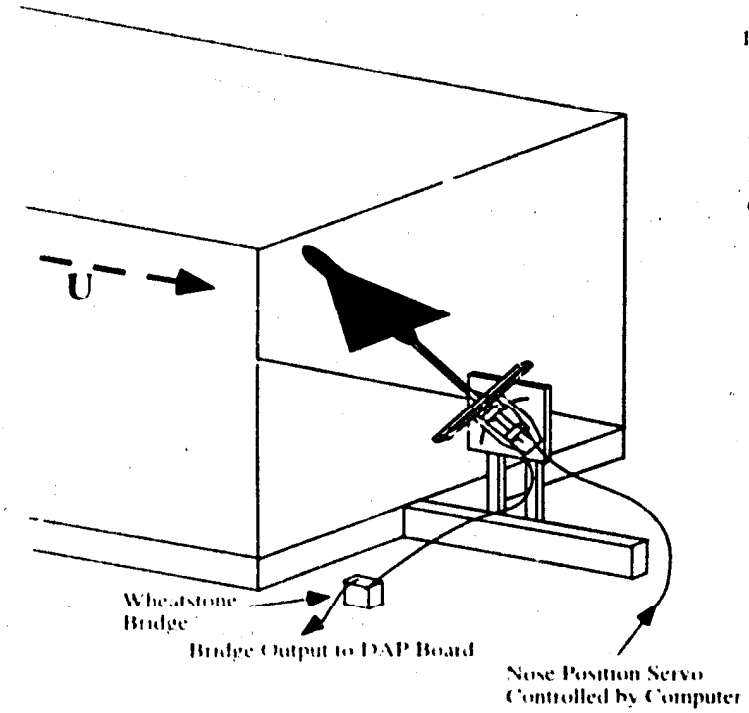

Figure 7 Schematic of Model Mounted on Roll Balance

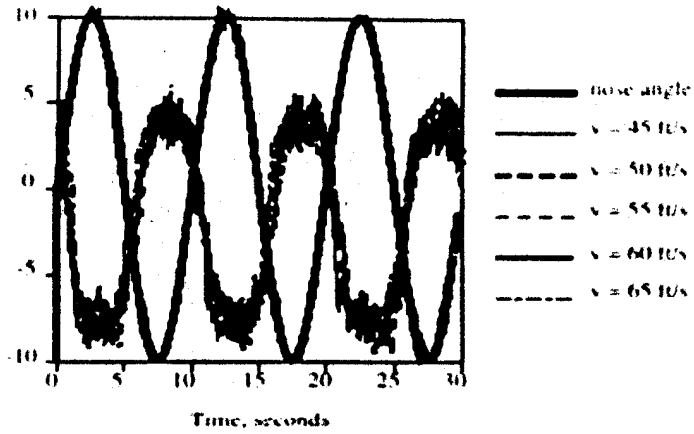

Figure 8a Rolling Moment Coefficient Response to Sine Wave Motion at 0.1 Hz at 40 deg angle of attack Axis is nose angle in deg and Cm * 100

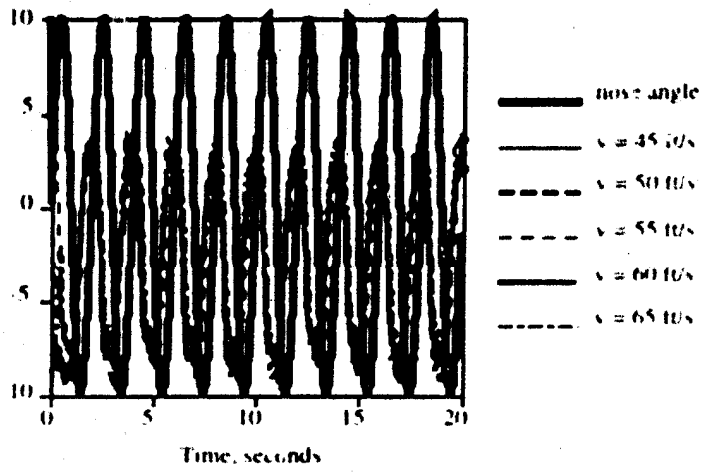

Figure 8b Rolling Moment Coefficient Response to Sine Wave Motion at 0.5 Hz at 40 deg angle of attack Axis is nose angle in deg and Cm * 100

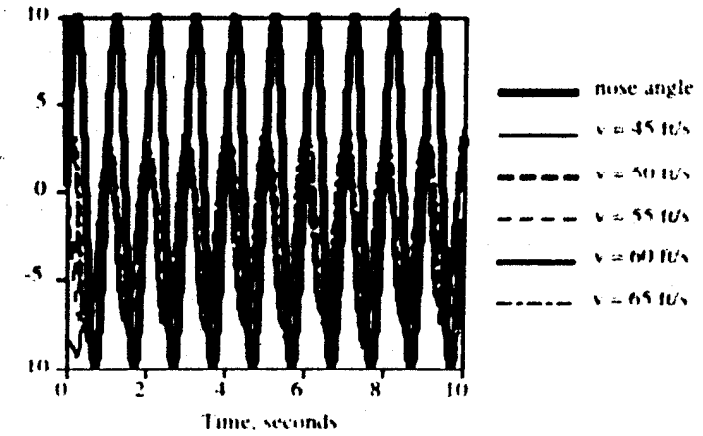

Figure 8c Rolling Moment Coefficient Response to Sine Wave Motion at 1.0 Hz at 40 deg angle of attack Axis is nose angle i deg and Cm * 100

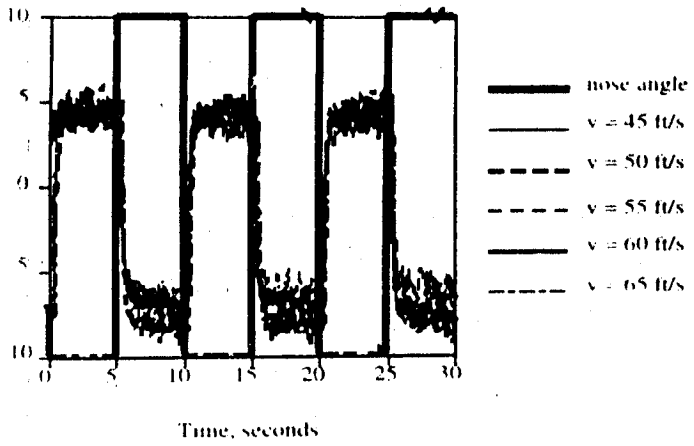

Figure 9a: Rolling Moment Coefficient Response to Square Wave Motion at 0.1 Hz at 40 deg. angle of attack. Axis is nose angle in deg. and Cm * 100

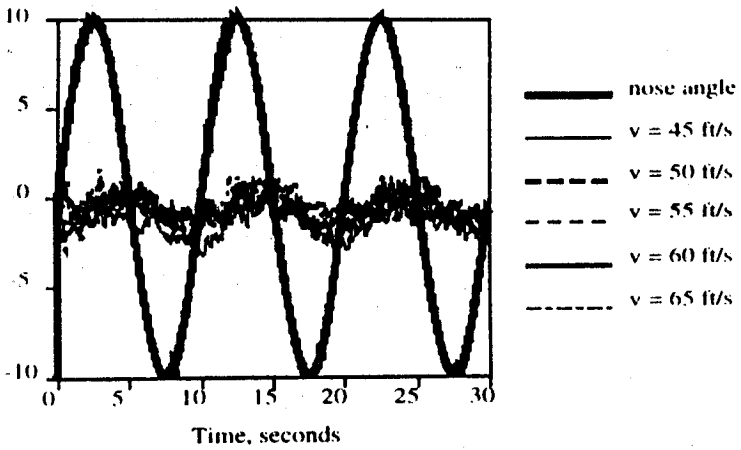

Figure 10a: Rolling Moment Coefficient Response to Sine Wave Motion at 0.1 Hz at 35 deg. angle of attack. Axis is nose angle in deg. and Cm * 100

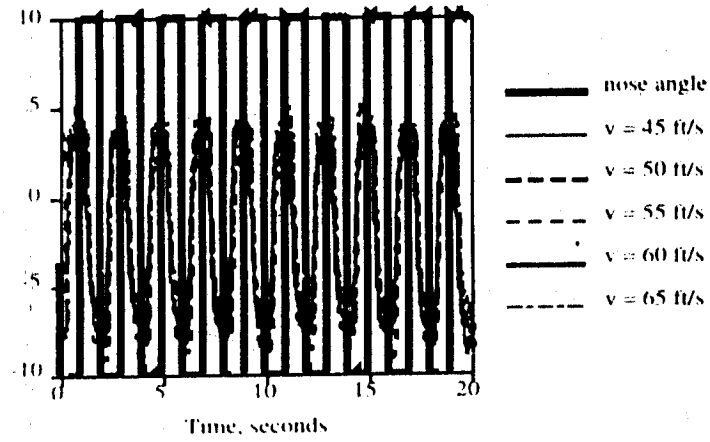

Figure 9b: Rolling Moment Coefficient Response to Square Wave Motion at 0.5 Hz at 40 deg. angle of attack. Axis is nose angle in deg. and Cm * 100

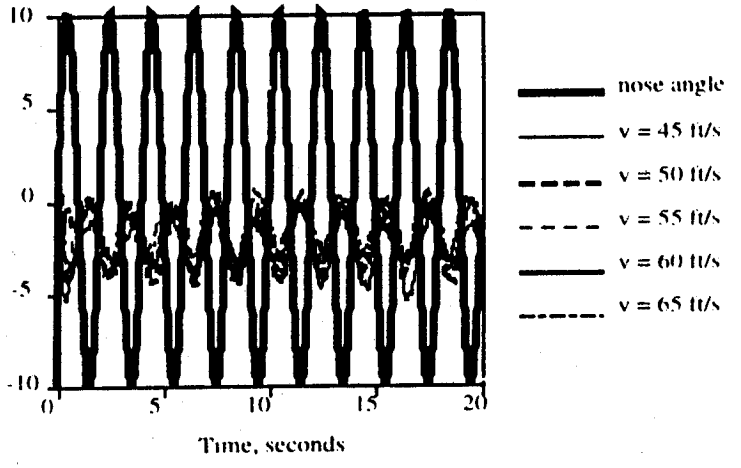

Figure 10b: Rolling Moment Coefficient Response to Sine Wave Motion at 0.5 Hz at 35 deg. angle of attack. Axis is nose angle in deg. and Cm * 100

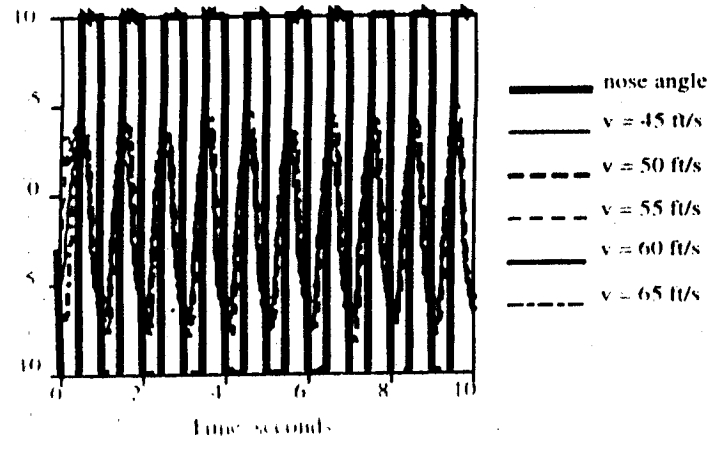

Figure 9c: Rolling Moment Coefficient Response to Square Wave Motion at 1.0 Hz at 40 deg. angle of attack. Axis is nose angle in deg. and Cm * 100

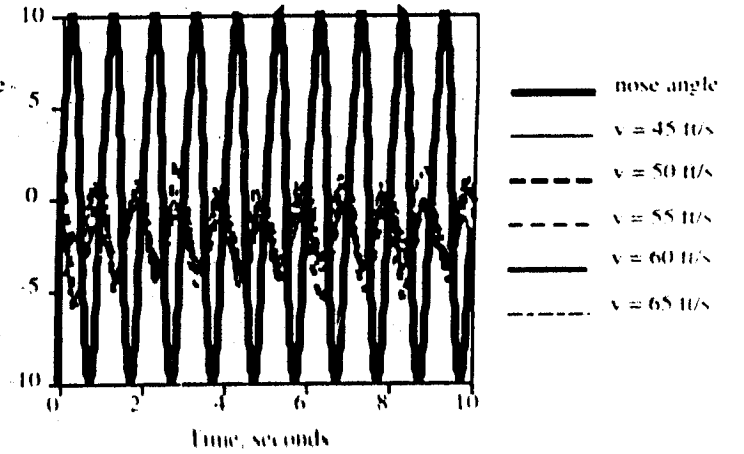

Figure 10c: Rolling Moment Coefficient Response to Sine Wave Motion at 1.0 Hz at 35 deg. angle of attack. Axis is nose angle in deg. and Cm * 100

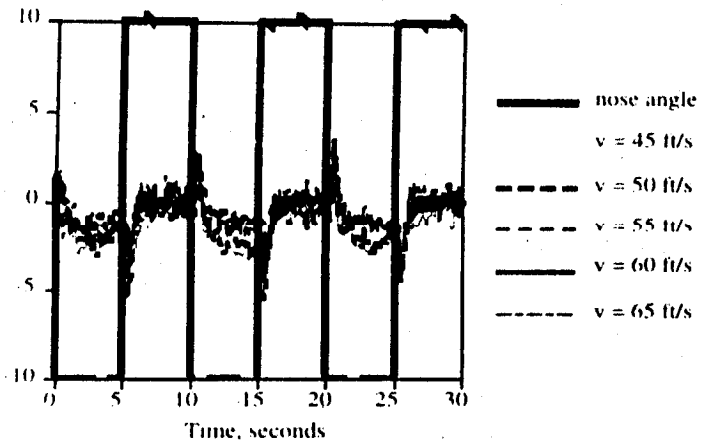

Figure 11a: Rolling Moment Coefficient Response to Square Wave Motion at 0.1 Hz at 35 deg. angle of attack. Axis is nose angle in deg. and Cm * 100

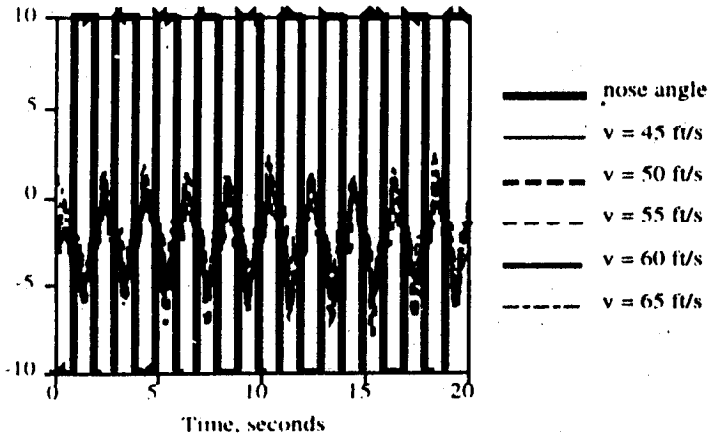

Figure 11b: Rolling Moment Coefficient Response to Square Wave Motion at 0.5 Hz at 35 deg. angle of attack. Axis is nose angle in deg. and Cm * 100

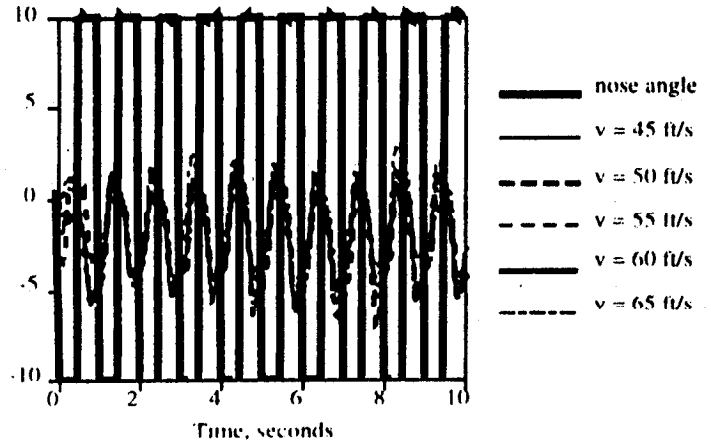

Figure 11c: Rolling Moment Coefficient Response to Square Wave Motion at 1.0 Hz at 35 deg. angle of attack. Axis is nose angle in deg. and Cm * 100

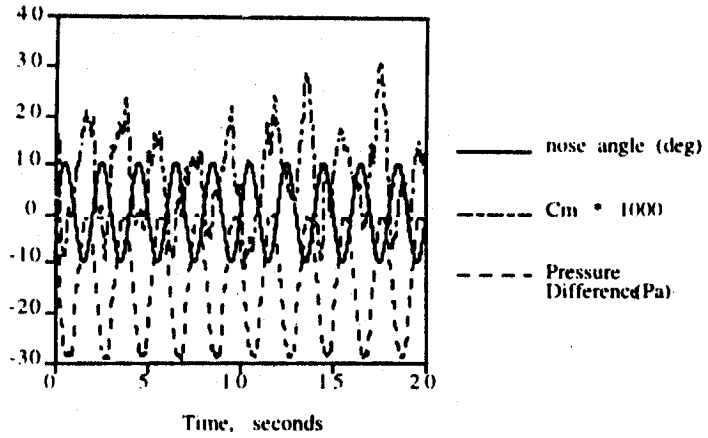

Figure 12a: Pressure Difference and Moment Response to Sine Wave Nose Excitation at 0.5 Hz, 35 deg. Angle of Attack, and 13.6 m/s Freestream Velocity

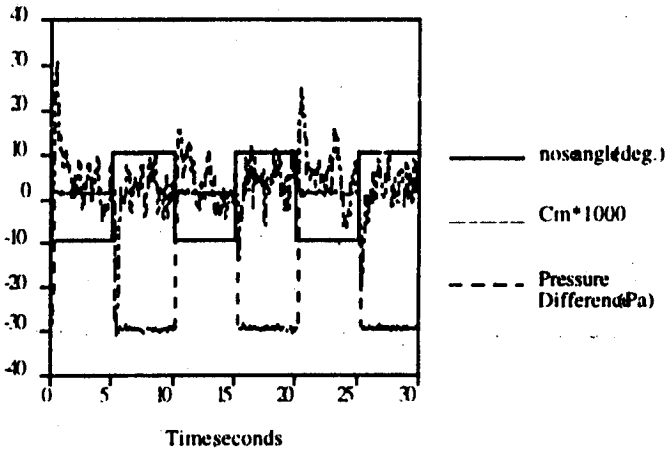

Figure 12b: Pressure Difference and Moment Response to Square Wave Nose Excitation at 0.1 Hz, 35 deg. Angle of Attack, and 13.6 m/s Freestream Velocity

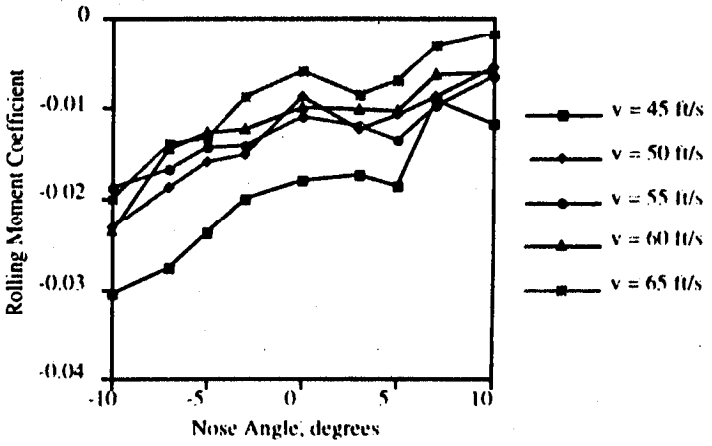

Figure 13a: Rolling Moment Coefficient vs. Nose Position at Various Speeds at 35 deg. Angle of Attack

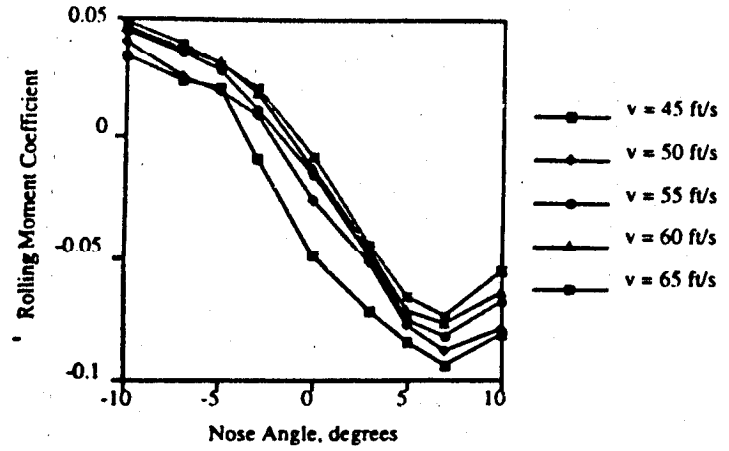

Figure 13b: Rolling Moment Coefficient vs. Nose Position at Various Speeds at 40 deg. Angle of Attack

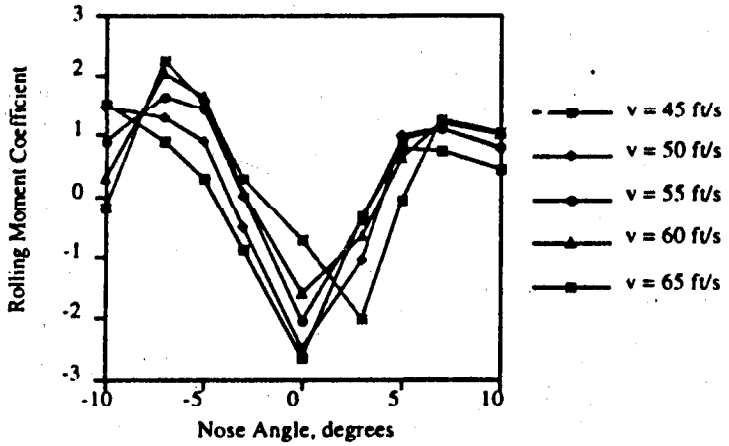

Figure 13c: Rolling Moment Coefficient vs. Nose Position at Various Speeds at 45 deg. Angle of Attack

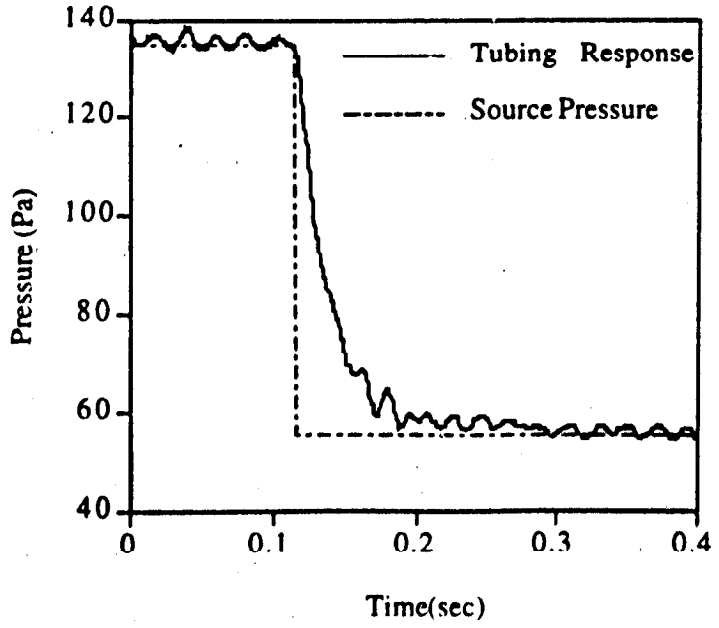

Figure 14: Response of the Pressure Sensing System to a Sudden Pressure Change